Carbohydrate Polymers 112 (2014) 502–511

Contents lists available at ScienceDirect

Carbohydrate Polymers

journal homepage: www.elsevier.com/locate/carbpol

Preparation and characterization of galactosylated alginate–chitosan oligomer microcapsule for hepatocytes microencapsulation

Meng Tian[a], Bo Han[b,c], Hong Tan[d], Chao You[a,*]

[a] Department of Neurosurgery, West China Hospital, Sichuan University, Chengdu 610041, Sichuan, PR China
[b] Department of Surgery, Keck School of Medicine, University of Southern California, Los Angeles, CA 90032, USA
[c] Department of Biomedical Engineering, University of Southern California, Los Angeles, CA 90032, USA
[d] College of Polymer Science and Engineering, State Key Laboratory of Polymer Materials Engineering, Sichuan University, Chengdu 610065, Sichuan, PR China

ARTICLE INFO

Article history:
Received 19 February 2014
Received in revised form 10 June 2014
Accepted 11 June 2014
Available online 19 June 2014

Keywords:
Galactosylated alginate
Microcapsule
Mechanical stability
Selective permeability
Microenvironment
Hepatocytes

ABSTRACT

Galactosylated alginate (GA)–chitosan oligomer microcapsule was prepared to provide a sufficient mechanical stability, a selective permeability and an appropriate three-dimensional (3D) microenvironment for hepatocytes microencapsulation. The microcapsule has a unique asymmetric membrane structure, with a dense layer located in the inner surface and gradually decreasing toward the outside surface. The stable microcapsule was obtained when GA lower than 50%, while the permeability was increased with increasing of GA. A balance between mechanical stability and permeability was achieved through modulating membrane porosity and thickness. The optimal microcapsule displays a selective permeability allowing efficient transport of human serum albumin while effectively blocking immunoglobulin G. Hepatocytes exhibited high and long term viability (>92%), proliferability, multicellular spheroid morphology, and enhancement of liver-specific functions in the microcapsule wherein galactose moieties present chemical cues to support cell–matrix interactions while the 3D structure of the microcapsule behaves physical cues to facilitate cell–cell interactions.

1. Introduction

Cell microencapsulation, a promising technology which is generally based on the immobilization of cells within a microcapsule surrounded by a semipermeable membrane, has been considered potentially therapeutic strategy for the treatment of a variety of diseases including diabetes, liver failure, cancer, as well as central nervous system and cardiovascular diseases (Hernández, Orive, Murua, & Pedraz, 2010). The membrane of the microcapsule is expected to provide not only sufficient mechanical stability that facilitates their production, handling, and use in applications involving shear force such as in in vitro perfusion bioreactors and in vivo implantation conditions, but also selective permeability that permits the diffusion of oxygen, nutrients, waste metabolites, and the therapeutic molecules of interest while excluding host antibodies and T-cells, thus protecting the encapsulated cells from the host immune system. Besides mechanical and selective permeable considerations, an ideal microcapsule should also be biocompatible, prepared in mild conditions, and provide an appropriate three-dimensional (3D) microenvironment for encapsulated cells to form tissue-like spheroids and maintain their differentiated functions. However, none of the existing microcapsules can satisfy all of these requirements.

Alginate based microcapsules are nowadays the most widely studied for cell microencapsulation due to their apparent biocompatibility and mild conditions of preparation (Goh, Heng, & Chan, 2012). These microcapsules are formed through a polyelectrolyte complexation reaction between an alginate core and a surrounded polycation layer such as poly-L-lysine, poly-L-ornithine, chitosan, lactose modified chitosan, and so on (Lim & Sun, 1980; Murua et al., 2008; Muzzarelli, 2009a). Nevertheless, the resulting microcapsules exhibit low mechanical resistance and poor stability, which shows the limited success in industrial and medical applications (Breguet, Gugerli, Pernetti, Stockar, & Marison, 2005). Instead of the traditional high molecular weight polycations, the use of chitosan oligomer permits the formation of microcapsules having good mechanical stability, and in particular the preparation is carried out in a one-step procedure under physiological conditions (Bartkowiak & Hunkeler, 1999; Muzzarelli, 2009b), which represents a strong advantage over the other microcapsules. However, this microcapsule has a permeability lower than 30% when diffusion of dextran with a molecular weight of 70 kDa, a molecular size

* Corresponding author. Tel.: +86 28 85422972; fax: +86 28 85422136.
E-mail address: Youchao@vip.126.com (C. You).

http://dx.doi.org/10.1016/j.carbpol.2014.06.025
0144-8617/

similar to that of albumin, indicating that the permeability of the microcapsule is required to be improved for cell microencapsulation.

Microcapsule can provide a 3D microenvironment for encapsulated cells to mimic their in vivo environment in vitro, since it has a liquid core, in which cells can grow freely surrounded by a semipermeable membrane. The presence of a 3D microenvironment that recapitulates various aspects of the in vivo microenvironment such as cell–matrix and cell–cell interactions has been reported to greatly improve the cell functions in vitro (Cho et al., 2006; Huang, Zhang, Wang, Wang, & Tang, 2012; Yang, Gotob, Ise, Cho, & Akaike, 2002). Alginate derived from brown algae as an important naturally occurring carbohydrate polymer has been widely used in a variety of biomedical applications due to its biocompatibility and nontoxicity (Lee & Mooney, 2012; Xu et al., 2013). However, its lack of specific interactions with cells limited its use as an appropriate 3D microenvironment for cells. For example, hepatocytes encapsulated in alginate/Ca^{2+} microcapsules exhibited low viability and liver functions due to the lack of cell–matrix and cell–cell interactions (Yang et al., 2002).

Hepatocytes are anchorage-dependent cells and have the tendency to form aggregates spontaneously in vitro. When enzymatically isolated from the liver and cultured in monolayer or suspensions, they rapidly lose adult liver morphology and differentiation functions. Recent study on maintenance of liver-specific functions of hepatocytes was focused on introduction of galactose moieties as asialoglycoprotein-receptor (ASGP-R) ligands to improve the hepatocytes anchorage and the interaction of hepatocytes with scaffold materials (Cho et al., 2006; Chu et al., 2009; Chung et al., 2002; Fan, Shang, Yuan, & Yang, 2010; Gotoh, Ishizuka, Matsuura, & Niimi, 2011; Seo, Choi, Akaike, Higuchi, & Cho, 2006a; Seo, Kim, Choi, Akaike, & Cho, 2006b; Wang et al., 2010; Yang et al., 2012). It was reported that hepatocytes attached onto galactosylated surface changed from spreading to round shapes with an increase of galactose moieties concentration and maintained the differentiated functions with promoting spheroids formation, which was shown to maintain a tissue-like cytological structure and sustain higher levels of many differentiated functions than hepatocytes cultured as monolayers (Yang et al., 2002). Therefore, it has been known that galactose moieties can guide hepatocyte adhesion through receptor-mediated interaction and enhance cell functions such as albumin secretion and urea synthesis.

In this work, a combination of chitosan oligomer and galactose moieties modification was investigated in order to provide a microcapsule with mechanical stability, selective permeability, and appropriate 3D microenvironment for hepatocytes microencapsulation. The use of chitosan oligomer permits the formation of microcapsules in a one-step procedure under physiological conditions, which will improve the viability of the encapsulated cells. The modification with galactose moieties is used to provide cell–matrix interactions for hepatocytes adhesion and enhance cell functions. Moreover, the introduction of galactose moieties to the backbone of alginate will enhance the permeability of the microcapsule, since part of carboxylic groups along the chains of alginate was replaced. Therefore, the mechanical stability and permeability can be modulated to achieve a balance. Finally, cell viability, proliferation, morphology and functions such as albumin secretion and urea synthesis of the hepatocytes within the microcapsule were studied.

2. Materials and methods

2.1. Materials

Sodium alginate (viscosity: 495.0 cps at 25 °C) was obtained from Zhejiang Jingyan Biotechnology Co. Ltd (China). Chitosan oligomer ($Mn < 3000$) was purchased from Zhejiang Aoxing Biotechnology Co., Ltd. (China). Lactobionic acid and 1-ethyl-3-(3-dimethy-lamino-propyl) carbodiimide (EDC) were supplied by Sigma-Aldrich (USA). *N*-hydroxylsuccinimide (NHS) was purchased from Pierce (USA). RPMI-1640 and phenol red-free RPMI-1640 media were obtained from Gibco (USA). Fetal bovine serum (FBS) was purchased from HyClone (USA). Fluorescein isothiocyanate labeled human serum albumin (FITC-HAS), fluorescein isothiocyanate labeled human immunoglobulin G (FITC-IgG), and urea nitrogen kit were from Nanjing Jiancheng Bioengineering Institute (China). Live/dead assay and Alamer blue assay kits were purchased from Invitrogen (USA). Human albumin ELISA quantitation kit was obtained from Bethyl Laboratories (USA).

2.2. Synthesis of galactosylated alginate (GA)

As shown in Fig. 1, the synthesis of GA was carried out by coupling alginate with galactose moiety in the presence of EDC and NHS in *N*,*N*,*N*-tetra-methylethylenediamine (TEMED) buffer as described elsewhere with a minor modification (Chiari, Cretich, Riva, & Casali, 2001; Fan et al., 2010; Wang et al., 2010; Yang et al., 2002). Briefly, 10 g of lactobionic acid was dissolved in 65 ml boiling 2-methoxyethanol, followed by the addition of 40 ml toluene, which caused the precipitation of a white solid. Lactobionic lactone was obtained by distillation of the toluene and white solid mixture at 124 °C for three times. Then, 5 g of lactobionic lactone was refluxed with 30-fold excess ethylenediamine (29.4 ml) dissolved in 50 ml anhydrous methanol at 70 °C for 2 h. The monoamine terminated lactobionic lactone (L-NH_2) was precipitated with chloroform and the obtained precipitate was vacuum-dried. Finally, 1 g of L-NH_2 was added to a stirred solution of alginate sodium (1 g) in 100 ml of 50 mM TEMED (0.3 M NaCl, pH 6.5) containing EDC and NHS (EDC = 2.5 g, molar ratio NHS/EDC = 0.2) for 24 h. The resulting solution was dialyzed against distilled water for 7 days at room temperature and then lyophilized to obtain GA. The GA was characterized by Fourier transform infrared spectroscopy (FTIR, Nicolet 670, USA), ^{1}H nuclear magnetic resonance spectroscopy (^{1}H NMR, Bruker AV II—400 MHz, Switzerland), and elemental analysis (Vario EL III, Germany).

2.3. Preparation of microcapsule

The microcapsules were prepared by formation of polyelectrolyte complexes through carboxylic and amino groups of GA/alginate and chitosan oligomer, respectively. In brief, a mixture of GA and alginate with a stated ratio r (r = 0, 0.3, 0.5 and 1, where r is the ratio of GA weight to sum of alginate and GA weight in the mixture) was dissolved in 0.01 M phosphate-buffered saline (PBS) at a concentration of 1% (w/v). Then, 1 ml of GA/alginate solution was introduced into a 1 ml syringe with a 27 G flat-cut needle, and the solution was extruded into 50 ml of chitosan oligomer solution (0.8% (w/v), pH = 7.0) under gently agitation with a small magnetic bar. The extruded droplets were allowed to complex reaction for 5, 10, and 20 min to form membrane. The formed microcapsules were filtered, rinsed three times with PBS, and stored at 4 °C in PBS/0.01% sodium azide.

2.4. Microcapsule membrane observation

To observe the membrane of the microcapsule, the microcapsules were stained in 0.01% eosine/PBS for 30 min and then washed with PBS. Membrane structure and thickness were observed using a spinning disk confocal microscopy (Perkin Elmer, USA).

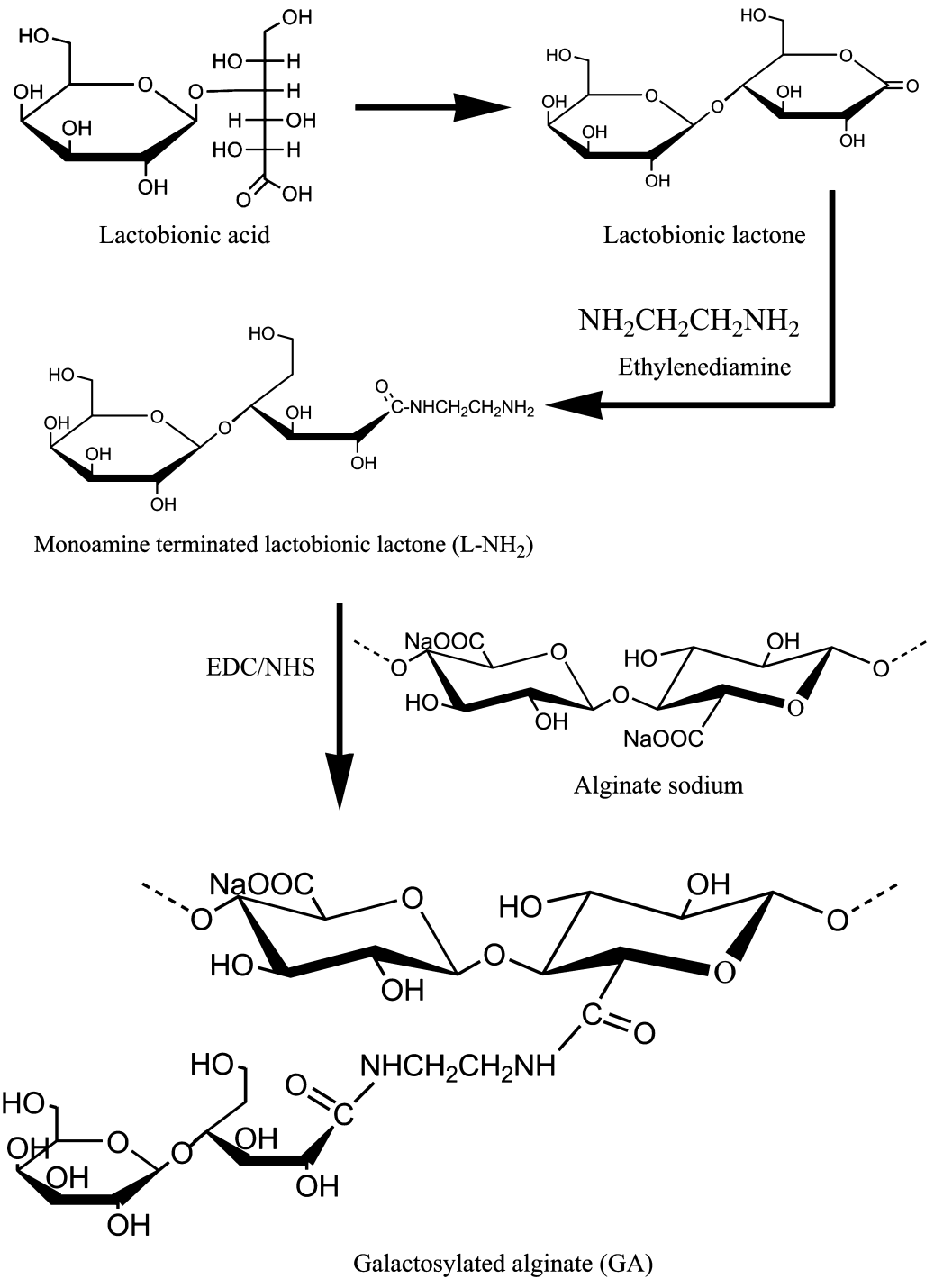

Fig. 1. The reaction route of GA.

2.5. Mechanical property of the microcapsule

Mechanical property of the microcapsules was determined by a shear force test (Yin et al., 2003). About 100 microcapsules prepared under the stated condition were added into a 6-well plate (Corning, USA). The microcapsules were equilibrated in 3 ml of PBS for 15 min. The plate was then immobilized on an orbital shaker (Model HY-5, Zhongda Instrument, China) and agitated with a frequency of 250 rpm at 37 °C. The percentage of ruptured microcapsules at various time points was counted with a phase contrast microscope (CKX41, Olympus, Japan).

2.6. Permeability of the microcapsule

Permeability of the microcapsule was investigated by examining the diffusion of FITC-HSA and FITC-IgG from microcapsules (Yin et al., 2003; Zhu et al., 2005). FITC-HAS and FITC-IgG were, respectively, dissolved in the stated ratio GA/alginate mixture solution with a concentration of 1 mg/ml and then the microcapsule was prepared as above description. For permeability assay, the microcapsules were quickly rinsed with PBS before they were placed into fresh PBS for measuring the release of FITC-HAS or FITC-IgG from the microcapsules. At the time point of 5, 10, 20, 40, 80, 120,

and 160 min, FITC-HAS or FITC-IgG released from the microcapsules into PBS were collected and analyzed on a spectrofluorometer (F-7000, Hitachi, Japan). The diffusion (%) was calculated based on the percentage of the amount of released FITC labeled protein over the initial amount of FITC labeled protein in the microcapsules.

2.7. Hepatocytes microencapsulation

Normal human hepatocytes, L02, were cultured as described previously (Tian et al., 2010). GA and alginate were sterilized with UV irradiation and dissolved with PBS to prepare GA/alginate mixture solutions. Hepatocytes were suspended in the mixture solution with a cell density of 1×10^6 cells/ml and extruded into a gently agitated chitosan oligomer solution sterilized with a 0.2 μm filter (Millipore, USA) to form microcapsules as above description. The microcapsules were harvested, washed with PBS, and subsequently cultivated in phenol red-free RPMI-1640 medium supplemented with 10% FBS, 100 μg/ml penicillin and 100 μg/ml streptomycin at 37 °C in a 5% CO_2 atmosphere, with medium changed every day. The cells in the microcapsule were observed under a phase contrast microscope (CKX41, Olympus, Japan).

2.8. Cell viability and proliferation

The viability of the encapsulated cells was determined using the live/dead assay kit from Invitrogen. Briefly, 1 μl of ethidium homodimer-1 and 0.25 μl of calcein acetoxymethyl ester from the kit were diluted with 500 μl RPMI-1640 without phenol red. The microcapsules were stained for 30 min at room temperature in the dark and imaged with a spinning disk confocal microscopy (Perkin Elmer, USA). Green (live cells) and red (dead cells) fluorescence images were collected separately and merged to determine cell viability as the ratio of viable cells to total cells counted.

The proliferation of the hepatocytes encapsulated in the microcapsule was determined using the Alamar Blue assay following the manufacturer's instructions. Briefly, phenol red free RPMI-1640 medium containing 10% Alamar Blue was added to each well containing microencapsulated cells and incubated for 4 h, and then 100 μl of the incubation medium was transferred into a 96 well plate. The absorbance of each well was determined using a microplate reader at a wavelength of 570 nm. The proliferation rates are presented as fold increase over the value of the absorbance obtained after the first day of culture (Tian et al., 2012).

2.9. Functional analysis of the microencapsulated hepatocytes

Albumin and urea synthesis were determined to evaluate the function of the microencapsulated hepatocytes. The medium was refreshed daily and the collected medium was centrifuged in 14,000 rpm for 10 min. The supernatant was stored at −20 °C for albumin assay. The amount of albumin secreted into the medium was quantified using a human albumin ELISA quantitation kit (Bethyl Laboratories, USA) under the conditions recommended by the manufacturer. To assess the urea synthesis function of the cells microencapsulated, the culture medium was replaced with fresh phenol red-free RPMI-1640 medium containing 5 mm NH_4Cl. The cells were cultured in this medium for 120 min, before the medium was again replaced with the normal medium. The collected medium was tested for urea production using a Urea Nitrogen Kit (Tian et al., 2010). Briefly, each collected medium (20 μl) was mixed in a tube with 1 ml of blood urea nitrogen (BUN) acid reagent and 1 ml of BUN color reagent, and then heated in boiling water for exactly 15 min. The tubes were allowed to cool in a water bath for about 5 min. The optical density of each sample in the tube was determined using an ultraviolet-visible spectrophotometer at a wavelength of 520 nm. Known quantities of urea nitrogen standards were used to establish the standard curve.

2.10. Statistical analysis

Results were presented by mean ± standard deviation (M ± S.D.). Each result was statistically analyzed by SPSS 13.0. A Student's *t*-test was performed to determine the statistical significance between experimental groups. The values of $p < 0.05$ were considered statistically significant.

3. Results and discussion

3.1. Synthesis and characterization of GA

In the FTIR spectra shown in Fig. 2A, lactobionic acid exhibited characteristic absorption at 1742 cm^{-1}, which was attributed to the carbonyl stretching (C=O) of carboxylic groups. After be dehydrated, the absorptions of carbonyl groups increased significantly, indicating the formation of lactobionic lactone. The characteristic absorption at 1650 of L-NH_2 is assigned to amide I. For the GA, the absorption at 1621 cm^{-1} is hard to assign, since the carbonyl groups of alginate sodium exhibit characteristic absorptions at 1609 cm^{-1}. However, a new peak at 1546 cm^{-1} was observed, which was contributed to amide II, indicating amide bond formation.

In the ^{1}H NMR spectrum of lactobionic acid (Fig. 2B), the signals at 4.46, 4.36, 4.27, 4.1, 3.9, 3.8, 3.75, 3.70, 3.66, 3.6, and 3.4 ppm are assigned to H-9, H-1, H-5, H-2, H-4, H-6, H-7, H-8, H-10, H-11, and H-3 of the lactobionic acid, respectively (Chen et al., 2012; Kang et al., 2005; Matute et al., 2013; Villa et al., 2013; Zhang, Tang, & Yin, 2013; Zheng et al., 2012; Zhou et al., 2013). In comparison with the ^{1}H NMR spectrum of lactobionic acid, the signals assigned to H-1 and H-4 of L-NH_2, respectively, shifted to 4.63 and 1.25 ppm. The signals at 3.5 and 3.25 ppm are, respectively, assigned to H-12 and H-13 of L-NH_2, which evident conjugation of ethylenediamine. In the ^{1}H NMR spectrum of GA, the signals assigned to H-12 can be identified. However, the most of the characteristic peaks of L-NH_2 and alginate both appeared in the range of 3.5–4.5 ppm and overlapped, which resulted in the difficulty to assign all galactose residue in the GA (Fan et al., 2010; Wang et al., 2010; Yang et al., 2002). In addition, there are more peaks appeared in the GA. To examine the possibility that these peaks result from the incomplete replacement of the activated ester, the ^{1}H NMR spectrum of the EDC was also recorded. Indeed, two characteristic peaks could be easily identified in the GA for EDC. The one is the triplet located in ~1.0 ppm, which belongs to CH_3 group marked H-6 in the EDC due to a CH_2 group nearby. The other is the quartet located in ~3.0 ppm which was assigned to H-3 of the CH_2 in the EDC due to four neighbor protons (Davidovich-Pinhas, Harari, & Bianco-Peled, 2009).

From the FTIR and ^{1}H NMR results, it can be concluded that besides the coupling of galactose moieties some EDC molecules remain attached to the alginate backbone. This phenomenon is similar to that reported by Davidovich-Pinhas et al. (2009). To estimate the content of galacotose moieties and EDC, the element analysis was carried out (Supplementary data). The content of galactose moieties in the GA was evaluated by element analysis of carbon, hydrogen and nitrogen content and it showed that 20.0% of carboxylic groups in alginate was replaced by galactose moieties. Accordingly, 8% of EDC was found to remain attached to alginate backbone. Together, a total of 28% of carboxylic groups in alginate was replaced.

3.2. Microcapsule preparation

The microcapsule was formed by polyelectrolyte complexes between GA/alginate and chitosan oligomer. The GA/alginate and

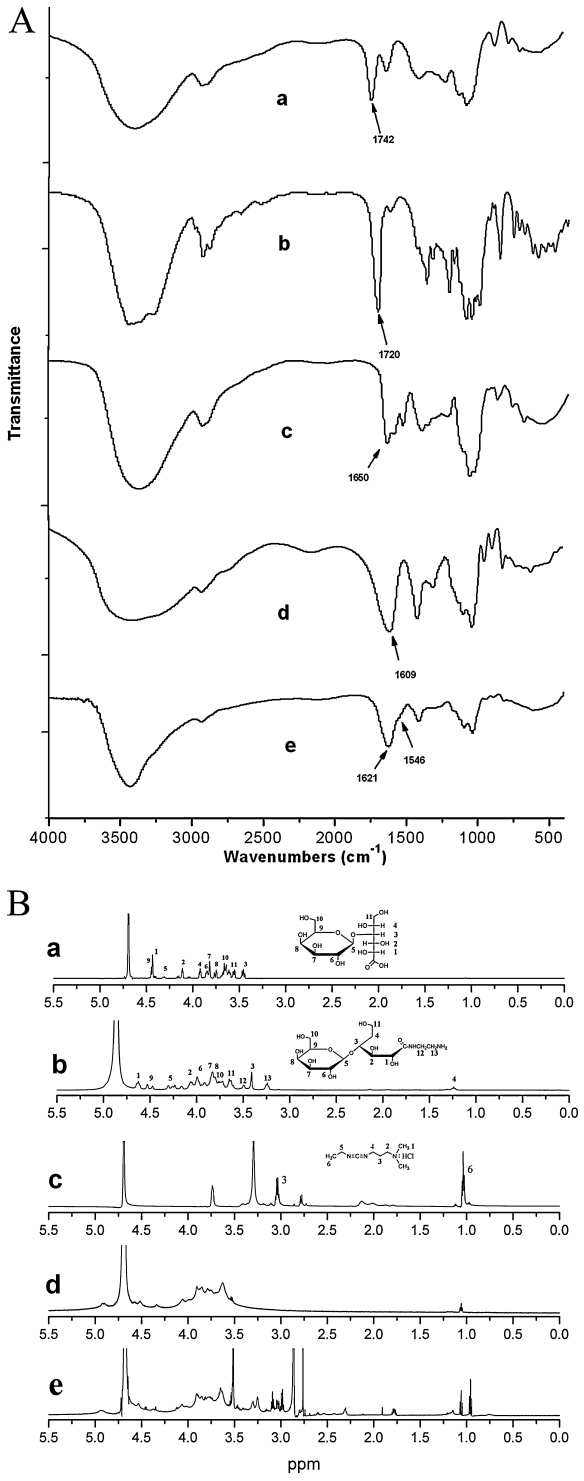

Fig. 2. (A) FTIR spectra of lactobionic acid (a), lactobionic lactone (b), L-NH_2 (c), sodium alginate (d), and GA (e). (B) ^{1}H NMR spectra of lactobionic acid (a), L-NH_2 (b), EDC (c), sodium alginate (d), and GA (e).

chitosan oligomer concentration were 1% and 0.8%, respectively. The effects of the ratio of GA to alginate and reaction time on the microcapsule are shown in Table 1. The microcapsule can not be formed when the mixture containing 100% GA ($r = 1$) was extruded into the chitosan oligomer solution. The formed microcapsule prepared with $r = 0.5$ was too soft and easily broken. The stable microcapsule was obtained when r is 0.3 or 0. The prepared microcapsules are shown in Fig. 3A, with a diameter of about 1 mm.

Table 1
Microcapsules prepared with different GA ratios (r is the ratio of GA weight to sum of alginate and GA weight) and reaction time.

GA ratio (r)	Membrane-forming time (min)	Gross observation	Microcapsule size (mm)
1	5	Non-forming	–
	10	Non-forming	–
	20	Non-forming	–
0.5	5	Soft, easily broken	–
	10	Soft, easily broken	–
	20	Soft, easily broken	–
0.3	5	Stable	1.1 ± 0.2
	10	Stable	1.0 ± 0.2
	20	Stable	1.1 ± 0.2
0	5	Stable	1.1 ± 0.2
	10	Stable	1.1 ± 0.2
	20	Stable	1.0 ± 0.2

Microcapsule formation is influenced by various factors, including polyanion and polycation concentration, the pH, and the ionic strength (Rosas-Flores, Ramos-Ramírez, & Salazar-Montoya, 2013). For cell encapsulation, physiological conditions were required to maintain the viability of living cells. Thus, an additional preparation condition was set at pH 7.0 in PBS, since chitosan oligomer is soluble due to a reduction of hydrogen-bond interactions (Domard, 2011). On the other hand, it was reported that the alginate/chitsoan oligomer microcapsule has a permeability lower than 30% when diffusion of dextran with a molecular weight of 70 ka (Bartkowiak & Hunkeler, 1999). Therefore, the permeability of the microcapsule is required to be improved for hepatocytes microencapsulation. In the present study, 1% alginate or GA/alginate concentration was chosen based on previous reports in which higher alginate concentration resulted in higher charge density, denser membrane, and lower permeability. It was also important to form microcapsules using low concentrations of chitosan oligomer because the droplets of alginate or GA/alginate would float on the surface of the chitosan oligomer solution with high concentration due to high viscosity. The chitosan oligomer solution with 0.8% concentration was found to form microcapsule reliably when using 1% of alginate solution.

Although the microcapsule can be prepared with the pure alginate solution, the GA/alginate mixture solution with high GA ratio cannot form microcapsule. The reasons might be due to a decrease of negative charge density on the droplet surface, since 28% of carboxylic groups along the chains of alginate were replaced by galactose moieties or EDC as mentioned above, which resulted in weak polyelectrolyte complexes between GA and chitosan oligomer. This phenomenon was also present in preparation of other microcapsules, for instance, Yang et al. (2002) prepared a Ca^{2+} crosslinked microcapsule using a mixture of GA and alginate with a weight ratio of 1:1.

3.3. Membrane characterization

The confocal micrographs of the microcapsules are shown in Fig. 3B. All microcapsules exhibit an asymmetric membrane structure and coarse outside surfaces. A dense layer is located in the inner surface, and gradually decreases toward the outside surface. The membrane thickness of the microcapsule containing 30% GA is, respectively, 35 ± 6, 50 ± 5, and 61 ± 7 μm, which have no significant differences with that the microcapsule without GA at various time points. However, with the GA content increases to 50%, the membrane thickness decreases significantly ($p < 0.05$), with

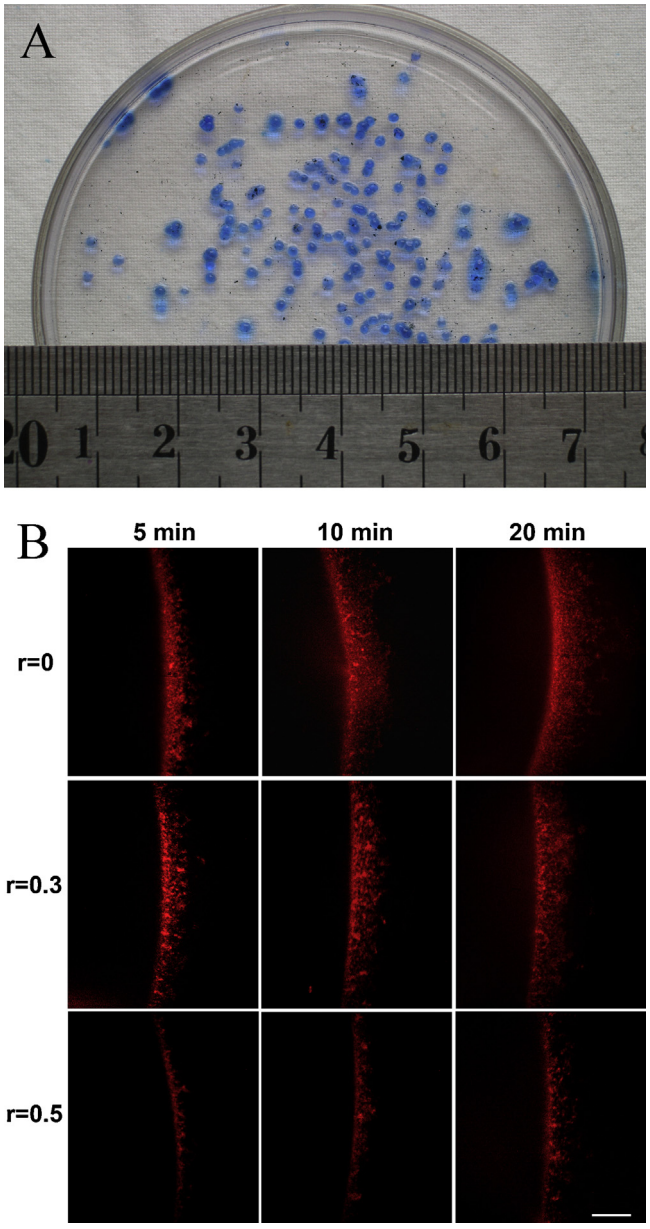

Fig. 3. (A) The appearance of galactosylated alginate–chitosan oligomer microcapsule ($r = 0.3$, $t = 10$ min, microcapsules were stained with methylene blue). (B) The confocal micrographs of the microcapsules prepared with $r = 0$, 0.3 and 0.5 after reaction time of 5, 10, and 20 min, respectively, scale bar, 50 μm.

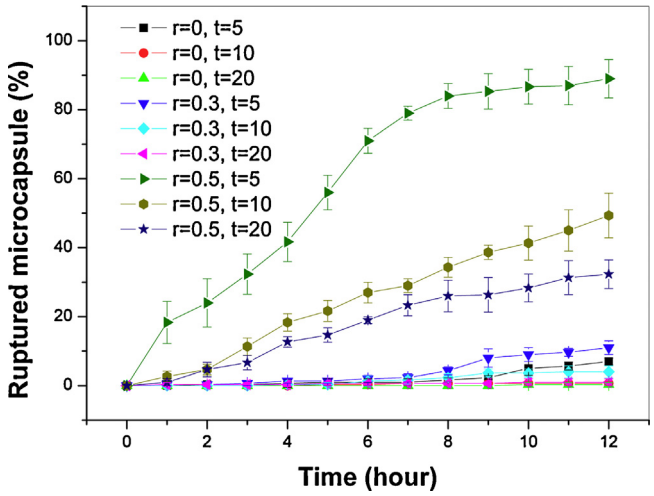

Fig. 4. The mechanical property of the microcapsule. Error bars represent means ± SD for $n = 3$.

thickness of 9 ± 3, 24 ± 5, and 32 ± 8 μm after reaction time of 5, 10, and 20 min, respectively.

Membrane structure and thickness are critical as they ultimately influence the properties of the microcapsule. The membrane structure can be divided into two major types, i.e., homogeneous and heterogeneous membrane (or termed symmetric and asymmetric membrane). For the classic alginate-poly-L-lysine microcapsule, the membrane structure can range from almost homogeneous to highly heterogeneous depending on the selected gelling ions, the conditions used for coating alginate microbeads by poly-L-lysine, and the effects of washing and storing of microcapsules (Strand, Morch, Espevik, & Skjak-Braek, 2003). In most cases, however, microcapsules prepared by utilizing a polyelectrolyte complexation reaction between two oppositely charged polysaccharides form an asymmetric membrane structure as a result of the phase separation process. The formed membrane exhibits an asymmetric membrane structure with a dense skin layer at the outside surface and decrease toward to the core of microcapsule. In our present work, it was found for the first time that the microcapsules have an asymmetric membrane structure, with a dense layer located in the inner surface and gradually decreasing toward the outside surface. This unique structure is different from the previously reported membrane structure in which skin layer commonly lacated in the outside surface (Bartkowiak, 2001; Bartkowiak & Hunkeler, 1999). Although the mechanisms underlying this phenomenon are not completely known, some reasons can be deduced from the process of membrane formation. First, after initial skin layer construction, the membrane grows slowly with time not only in the direction of alginate but also in the direction of chitosan oligomer, which was observed by using the analytical ultracentrifugation technique that alginate diffusion to the outside surface of the microcapsule through the large pores on the skin layer (Bartkowiak, 2001). Second, the microcapsule prepared from a pair of oppositely charged polysaccharides with relative low concentrations resulted in increase of the membrane porosity which has the benefit to increase the diffusion of alginate (Zhu et al., 2005). The membrane thickness of the microcapsule increased with the increase in reaction time, while at the same reaction time, the thickness decreased with the increase of GA content, which resulted from weak polyelectrolyte complexes between GA and chitosan oligomer due to part of carboxylic groups along the chains of alginate were replaced.

3.4. Properties of the microcapsule

Fig. 4 shows the mechanical stability of the prepared microcapsule. The rapture percentage of the microcapsule formed with 50% GA increases with the shaking time prolonged, with percentage of 89.0%, 50.0%, and 32.3% after 12 h of shaking, respectively, for membrane reaction of 5, 10, and 20 min, indicating poor mechanical stability. In contrast, both the microcapsules formed with 0% and 30% GA exhibited improved mechanical stability. In addition, it can be observed that the mechanical stability increased with the membrane thickness, with 4% and 1% rapture percentage, respectively, for the microcapsules formed with 30% GA with membrane thickness of 50 and 61 μm.

Due to the microcapsule formed with 50% GA exhibits poor mechanical stability, the permeability study focused on the microcapsule formed with 30% and 0% GA. As shown in Fig. 5A, the release profile of FITC-HSA from all the microcapsules exhibited two stages. The first stage would be one of rapid burst releases, in which about

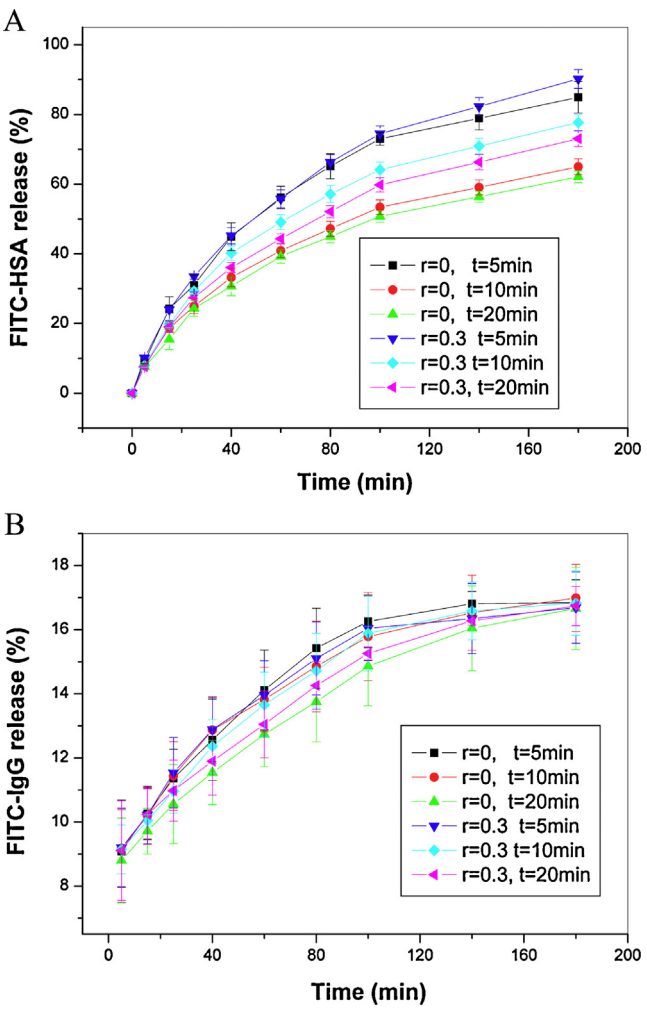

Fig. 5. The FITC-HSA (A) and FITC-IgG (B) release curves of the microcapsule. Error bars represent means ± SD for $n = 3$.

20% of FITC-HSA was released during the initial 20 min. The second stage would be one of slow releases, which was the extended release of the protein that was retarded in the microcapsule. The microcapsules formed with 5 min of membrane reaction showed faster release than that of microcapsule formed with 10 and 20 min membrane reaction. About 50% of FITC-HSA was released from the microcapsule in the initial 50 min, reaching 90% after 180 min. The microcapsules formed with 30% GA showed faster release than that of microcapsule formed without GA. After 180 min of release, both microcapsules containing GA formed with 10 and 20 min of membrane reaction time showed about 70% FITC-HSA release. In contrast, the release of the microcapsules formed without GA was about 60%. The release profile of FITC-IgG is illustrated in Fig. 5B. All microcapsules displayed similar release tendency, in which the release percentage was increased with the time increases during the initial 100 min, followed by approaching release equilibrium, with about 16% of FITC-IgG released from the microcapsule after 180 min. Considering that the microcapsules were immersed in the FITC-IgG solution and allowed to equilibrate resulting in the adsorption of IgG on the surface of the microcapsule before determination of the release profile, this suggests that the actual release amounts should be lower than that of the determined results.

For cell microencapsulation, the membrane of microcapsule should provide, on one hand, a sufficient mechanical resistance to bear both the forces exerted by the in vitro and in vivo environment, and on the other hand, a selective permeability to efficient transport of nutrients, oxygen, and the therapeutic molecules of interest while blocking the humoral component of the immune system such as IgG to induce undesired inflammatory and immune responses that can cause cell death (Zhang, Zhao, et al., 2013). The mechanical stability and permeability of the microcapsule are significantly dependent on the membrane thickness and porosity (Breguet et al., 2005; Ma et al., 2013; Zhu et al., 2005). A thick and dense membrane could provide good mechanical stability. Nevertheless, a thin and loose membrane reduces the diffusion distance and resistance and favors mass transfer. For modulating the properties of microcapsules, a balance has to be achieved between the membrane thickness and porosity, both of which varied greatly as a function of the preparation conditions, including polymer composition, concentration, and reaction time. Ma et al. (2013) studied the effect of membrane thickness (10, 15, 20, and 30 μm) on the strength and permeability of the alginate-poly-L-lysine-alginate microcapsule with the similar membrane porosity. The integrity ratio of microcapsules with 15, 20, and 30 μm membrane thicknesses maintained over 88% during culture time and there was no significant difference until 21 days. However, the microcapsules with 10 μm membrane thickness were too weak and with a rapture percentage more than 40%. In the aspect of permeability, the microcapsules with 10 and 20 μm membrane thickness showed higher BSA diffusion than others. So, the membrane thickness of 20 μm is optimal in this regard.

Alginate–chitosan oligomer microcapsule has shown good mechanical stability which mainly results from a significantly thicker membrane compared to other microcapsules (Bartkowiak, 2001); however, it in turn leads to a limited permeability when diffusion of dextran with a molecular weight of 70 ka, a molecular size similar to that of albumin. To modulate the microcapsule's permeability without significantly compromising the mechanical stability, efforts are made to increase the porosity of the membrane in this work. Meanwhile, the membrane thickness can be adjusted with reaction time. Here, we first prepared the microcapsule using a low concentrations of alginate and chitosan oligomer. The results showed the microcapsule exhibited a unique membrane structure and with a membrane thickness ranging between 30 and 60 μm, and the permeability of albumin was obviously improved. Moreover, the permeability was further improved when the microcapsule formation with GA, since part of carboxylic groups along the chains of alginate were replaced which resulted in weak polyelectrolyte complexes between alginate and chitosan oligomer and formation loose membranes. On the other hand, to protect the encapsulated cells from host immune destruction, the membrane of the microcapsule is expected to block the immune related molecules such as IgG (Zhang et al., 2012). The prepared microcapsule showed minor diffusion of IgG at initial stage and then approaching release equilibrium, suggesting the potential to be able to function as an immunoprotection barrier. Therefore, it can be concluded that the microcapsules have a selective permeability that allows not only effective transport of human serum albumin but minimized diffusion of the human immune system such as IgG to protect the encapsulated cells. Given an appropriate mechanical stability, the optimal microcapsule for cell encapsulation was prepared with 30% GA and 10 min reaction time, which has a membrane thickness of 50 μm and an albumin permeability of 70% after 180 min, approximately more than two times higher than that of previous report (Bartkowiak & Hunkeler, 1999).

3.5. Hepatocytes microencapsulation

The optimal microcapsule that prepared with 30% GA and 10 min reaction time was selected to encapsulate hepatocytes based on the above structure and property tests. The microcapsule formed with the same preparation conditions without GA was

used as a control. In both cases, the microcapsules were found to be stable and maintain their morphological integrity in the cell culture medium after 10 days, despite with a slight swelling, suggesting that the membrane of the microcapsule provides a sufficient mechanical stability for cell culture.

The viability of hepatocytes is shown in Fig. 6A and B. During 10 days culture, the cells in the GA-containing microcapsule displayed and maintained high viability more than 92%. The cells in the microcapsule without GA also exhibited high viability at the initial time, with 92% and 90% on day 2 and 5, respectively, and then the viability decreased to 86% on day 10. The cell viability is related with the preparation conditions, microcapsule size, permeability as well as 3D microenvironment (Tran et al., 2013). The preparation conditions have distinct effect on the viability of the encapsulated cells at the initial time. Although two-step procedure is widely used to prepare microcapsules such as alginate-poly-L-lysine and alginate–chitosan microcapsules, the encapsulated cells are confined in a noncultivating environment and exposed to many harmful elements (Yang et al., 2002). In contrast, one-step procedure used in this work is preferred due to operation in mind conditions and resulted in high viability. Small size and good permeability is beneficial to diffusion of oxygen, nutrients, waste metabolites which are essential for cell viability. The 3D microenvironment that recapitulates various aspects of the in vivo microenvironment such as cell–matrix and cell–cell interactions are also essential for hepatocyte viability. Cell–matrix interactions support cell anchorage and attachment, and cell–cell interactions result in multicellular aggregates with a structural organization mimicking the hepatocytes in vivo.

Cell proliferation within microcapsules was assessed using Alamar blue assay. As shown in Fig. 6C, after 10 days of culture, no cell proliferation was observed in the control group and a reduction of cell proliferation was observed on days 7 and 10 with decreases of about 12% and 18%, respectively. For the GA-containing microcapsule, the cells showed obvious proliferation on day 5 and then no significant increase was observed on day 7 and 10.

The morphology of hepatocytes encapsulated in the microcapsule is shown in Fig. 6D. In the microcapsule containing GA, the hepatocytes rapidly aggregated to form multicellular spheroids on day 2. With the time prolonged, the number and size of the spheroids increased, with diameters enlarged up to 100 μm, indicating a specific interaction of hepatocytes with GA. On the contrary, although most hepatocytes remained as single cells at the beginning culture, some of cells formed aggregates after 5 days within the control microcapsule. This is consistent with the previous reports (Seo et al., 2005; Yang et al., 2002), indicating that the 3D structure of the microcapsule support cell–cell interactions at some extent.

The albumin secretion and urea synthesis of the encapsulated hepatocytes within the GA–chitosan oligomer and the control microcapsule are shown in Fig. 7A and B. The albumin secretion of hepatocytes within the control microcapsule decreased during 10 days culture whereas the hepatocytes within GA–chitosan oligomer microcapsule showed increase of albumin secretion and higher than that of control after 7 days culture ($p < 0.05$). Similarly, the hepatocytes within GA–chitosan oligomer microcapsule showed higher urea synthesis than that of control after 5 days culture ($p < 0.05$).

Microcapsule should provide an appropriate 3D microenvironment for the encapsulated cells, not only for cell growth but also for maintaining and promotion of functional expressions. Hepatocytes are anchorage-dependent cells. In 2D cultures, the cells are unable to attach to the pure alginate matrix and to maintain survival due to the highly hydrated anionic surface that resists cell

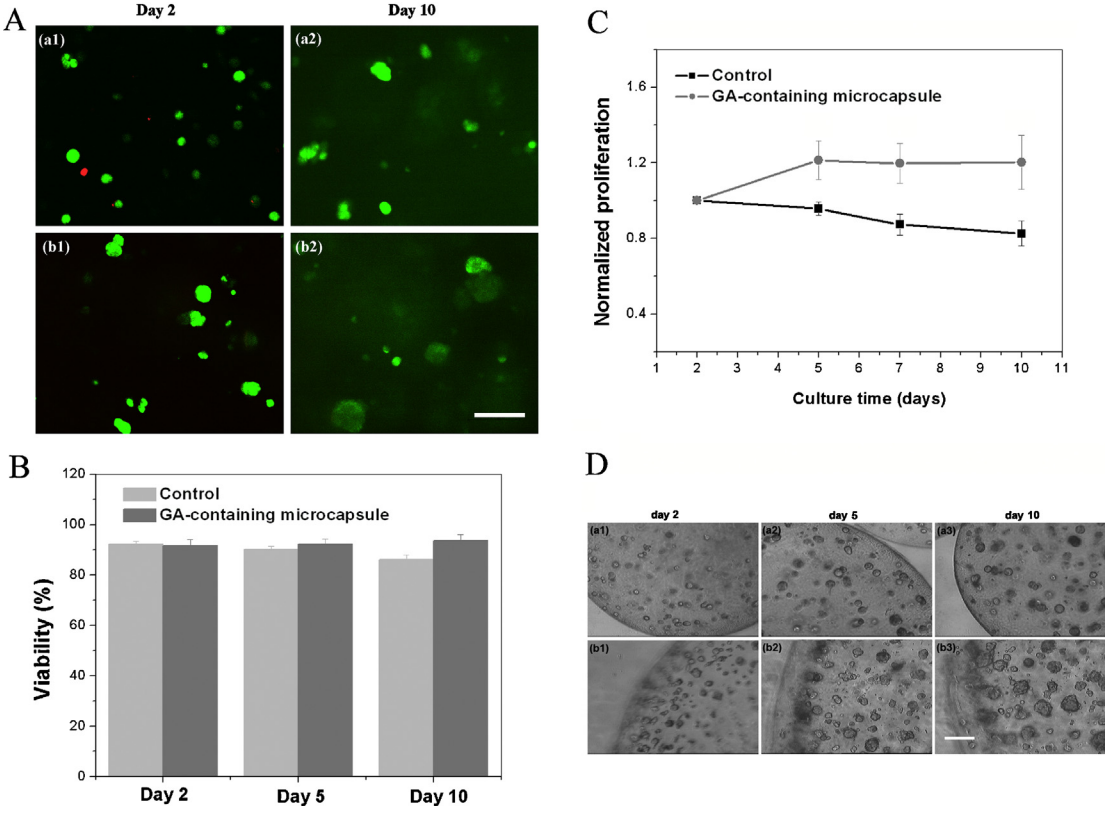

Fig. 6. (A) Live/dead staining of the hepatocytes in the GA-containing microcapsule (b1 and b2) and control (a1 and a2). Scale bar, 100 μm. (B) Viability of the hepatocytes in the microcapsule. Error bars represent means ± SD for $n = 3$. (C) Proliferation of the hepatocytes in the microcapsule. Error bars represent means ± SD for $n = 3$, * $p < 0.05$. (D) Phase-contrast micrographs of hepatocytes in the GA-containing microcapsule (b1–b3) and control (a1–a3). Scale bar, 100 μm.

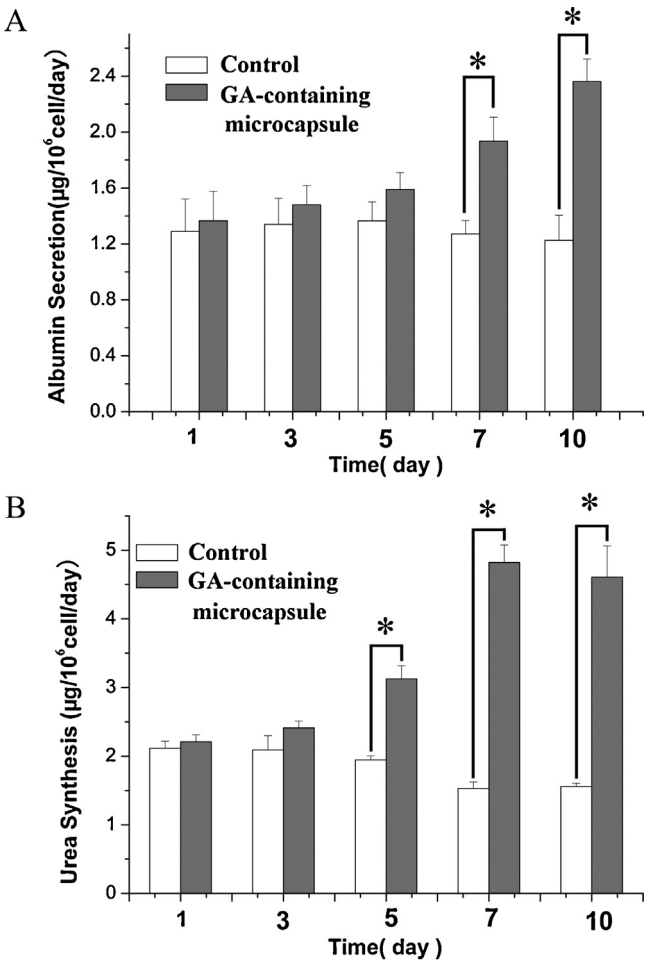

Fig. 7. The albumin secretion (A) and urea synthesis (B) of the hepatocytes in the microcapsule. Error bars represent means ± SD for $n = 3$, * $p < 0.05$.

adhesion and spreading (Seo et al., 2005). The situation changes when cells are exposed to 3D cultures wherein cells tend to aggregate to form cellular spheroids due to cell–cell interactions. In the native liver tissue, hepatocytes entrapped within a 3D microenvironment composed of cells and extracellular matrix (ECM), in which both cell–cell and cell–matrix interactions are facilitated to cell viability, proliferation as well as functions. To imitate this natural microenvironment in alginate microcapsule, cell–matrix interactions are emphasized in our study since cell–cell interactions are available in the microcapsules. One of the potential strategies employed to improve cell–matrix interactions is to couple bioactive molecules that are recognized by cell surface receptors. For example, many studies have reported that cell adhesion was regulated through immobilization of molecules containing RGD, a ligand for integrin cell adhesion receptors (Hersel, Dahmen, & Kessler, 2003). ASGP-R is abundantly located on the membrane surface of hepatocytes where it binds and endocytosis galactose-terminated glycoproteins. The use of coupling galactose moieties for ASGP-R recognition has been regarded as one of the most effective approaches to enhance cell–matrix interactions of hepatocytes (Nugraha et al., 2011; Qiu et al., 2012; Seo et al., 2005; Yang et al., 2012) and hepatocyte-targeted delivery vehicles (Craparo, Triolo, Pitarresi, Giammona, & Cavallaro, 2013; Li et al., 2013).

Herein, galactose moieties were coupled to the alginate backbone and then the microcapsule containing galactose moieties was prepared to provide a 3D microenvironment for hepatocytes that supports both cell–cell and cell–matrix interactions. The results showed that the hepatocytes encapsulated in the GA-containing microcapsule exhibited high and long term viability, proliferability, multicellular spheroid morphology, and enhancement of liver-specific functions. Therefore, it may be considered that the galactose moieties in the microcapsule supported hepatocytes growth and promoted the formation of hepatocyte spheroids, and then enhanced the cell functions. Unlike integrin, ASGP-R does not physiologically function as an adhesion receptor. The galactose moieties are more likely provide anchorage sites for hepatocytes, followed by incorporation of integrin mediated interactions involved in the recruitment of ECM proteins secreted by the hepatocytes during culture time. Ambury, Merry, and Ulijn (2011) recently revealed hepatocytes attached preferentially on the surface of polyethylene glycol acrylamide (PEGDA) hydrogel modified with galactose moieties. Moreover, they observed the secreted ECM proteins adsorption to the PEGDA and galactose moieties-PEGDA surfaces was similar. This indicated the proteins may attach in different orientations due to the sugars presented at the surface of the material. Taken together, GA-containing microcapsule was indicated to be favorable in providing a 3D microenvironment for hepatocytes microencapsulation, in which galactose moieties present chemical cues to support cell–matrix interactions for hepatocytes, while the 3D structure of the microcapsule behaves physical cues to facilitate cell–cell interactions.

4. Conclusion

The present study showed the microcapsule prepared with GA and chitosan oligomer having a GA content lower than 50% in the liquid core provide a sufficient mechanical stability, a selective permeability and an appropriate 3D microenvironment for hepatocytes microencapsulation. The microcapsule has a unique asymmetric membrane structure, with a dense layer located in the inner surface and gradually decreasing toward the outside surface. Hepatocytes in the microcapsule exhibited high and long term viability, proliferability, multicellular spheroid morphology, and enhancement of liver-specific functions. The results suggest that the prepared microcapsule should be a promising system for hepatocytes microencapsulation, which can be used in a variety of applications such as bioartificial liver, hepatocyte transplantation as well as drug assessment.

Acknowledgements

This work was partly supported by US NIH grant R41AR056177 and Translational Medicine Fund of West China Hospital of Sichuan University & Science and Technology Bureau of Chengdu ZH13013. The authors acknowledge Ernesto Barron, Douglas Hauser, and Hong Dan, researchers at Doheny Eye Institute of University of Southern California, for valuable suggestion and specimen characterization.

References

Ambury, R. F., Merry, C. L. R., & Ulijn, R. V. (2011). Sugar functionalised PEGA surfaces support metabolically active hepatocytes. *Journal of Materials Chemistry, 21*, 2901–2908.

Bartkowiak, A. (2001). Optimal conditions of transplantable binary polyelectrolyte microcapsules. *Annals of the New York Academy of Sciences, 944*, 120–134.

Bartkowiak, A., & Hunkeler, D. (1999). Alginate–oligochitosan microcapsules: A mechanistic study relating membrane and capsule properties to reaction conditions. *Chemistry of Materials, 11*, 2486–2492.

Breguet, V., Gugerli, R., Pernetti, M., Stockar, U., & Marison, I. W. (2005). Formation of microcapsules from polyelectrolyte and covalent interactions. *Langmuir, 21*, 9764–9772.

Chen, F., Tian, M., Zhang, D., Wang, J., Wang, Q., Yu, X., et al. (2012). Preparation and characterization of oxidized alginate covalently cross-linked galactosylated chitosan scaffold for liver tissue engineering. *Materials Science and Engineering C, 32*, 310–320.

Chiari, M., Cretich, M., Riva, S., & Casali, M. (2001). Performances of new sugar-bearing poly(acrylamide) copolymers as DNA sieving matrices and capillary coatings for electrophoresis. *Electrophoresis*, *22*, 699–706.

Cho, C. S., Seo, S. J., Park, I. K., Kim, S. H., Kim, T. H., Hoshiba, T., et al. (2006). Galactose-carrying polymers as extracellular matrices for liver tissue engineering. *Biomaterials*, *27*, 576–585.

Chu, X., Shi, X., Feng, Z., Gu, J., Xu, H., Zhang, Y., et al. (2009). In vitro evaluation of a multi-layer radial-flow bioreactor based on galactosylated chitosan nanofiber scaffolds. *Biomaterials*, *30*, 4533–4538.

Chung, T. W., Yang, J., Akaike, T., Cho, K. Y., Nah, J. W., Kim, S. I., et al. (2002). Preparation of alginate/galactosylated chitosan scaffold for hepatocyte attachment. *Biomaterials*, *23*, 2827–2834.

Craparo, E. F., Triolo, D., Pitarresi, G., Giammona, G., & Cavallaro, G. (2013). Galactosylated micelles for a ribavirin prodrug targeting to hepatocytes. *Biomacromolecules*, *14*, 1838–1849.

Davidovich-Pinhas, M., Harari, O., & Bianco-Peled, H. (2009). Evaluating the mucoadhesive properties of drug delivery systems based on hydrated thiolated alginate. *Journal of Controlled Release*, *136*, 38–44.

Domard, A. (2011). A perspective on 30 years research on chitin and chitosan. *Carbohydrate Polymers*, *84*, 696–703.

Fan, J., Shang, Y., Yuan, Y., & Yang, J. (2010). Preparation and characterization of chitosan/galactosylated hyaluronic acid scaffolds for primary hepatocytes culture. *Journal of Materials Science: Materials in Medicine*, *21*, 319–327.

Goh, C. H., Heng, P. W. S., & Chan, L. W. (2012). Alginates as a useful natural polymer for microencapsulation and therapeutic applications. *Carbohydrate Polymers*, *88*, 1–12.

Gotoh, Y., Ishizuka, Y., Matsuura, T., & Niimi, S. (2011). Spheroid formation and expression of liver-specific functions of human hepatocellular carcinoma-derived FLC-4 cells cultured in lactose–silk fibroin conjugate sponges. *Biomacromolecules*, *12*, 1532–1539.

Hernández, R. M., Orive, G., Murua, A., & Pedraz, J. L. (2010). Microcapsules and microcarriers for in situ cell delivery. *Advanced Drug Delivery Reviews*, *62*, 711–730.

Hersel, U., Dahmen, C., & Kessler, H. (2003). RGD modified polymers: Biomaterials for stimulated cell adhesion and beyond. *Biomaterials*, *24*, 4385–4415.

Huang, X., Zhang, X., Wang, X., Wang, C., & Tang, B. (2012). Microenvironment of alginate-based microcapsules for cell culture and tissue engineering. *Journal of Bioscience and Bioengineering*, *114*, 1–8.

Kang, I. K., Moon, J. S., Jeon, H. M., Meng, W., Kim, Y. I., Hwang, Y. J., et al. (2005). Morphology and metabolism of Ba–alginate encapsulated hepatocytes with galactosylated poly(allyl amine) and poly (vinyl alcohol) as extracellular matrices. *Journal of Materials Science: Materials in Medicine*, *16*, 533–539.

Lee, K. Y., & Mooney, D. J. (2012). Alginate: Properties and biomedical applications. *Progress in Polymer Science*, *37*, 106–126.

Li, C., Zhang, D., Guo, H., Hao, L., Zheng, D., Liu, G., et al. (2013). Preparation and characterization of galactosylated bovine serum albumin nanoparticles for liver-targeted delivery of oridonin. *International Journal of Pharmaceutics*, *448*, 79–86.

Lim, F., & Sun, A. M. (1980). Microencapsulated islets as bioartificial endocrine pancreas. *Science*, *210*, 908–910.

Ma, Y., Zhang, Y., Wang, Y., Wang, Q., Tan, M., Liu, Y., et al. (2013). Study of the effect of membrane thickness on microcapsule strength, permeability, and cell proliferation. *Journal of Biomedical Material Research, A*, *101A*, 1007–1015.

Matute, A., Cardelle-Cobas, A., García-Bermejo, A., Montilla, A., Olano, A., & Corzo, N. (2013). Synthesis, characterization and functional properties of galactosylated derivatives of chitosan through amide formation. *Food Hydrocolloids*, *33*, 245–255.

Murua, A., Portero, A., Orive, G., Hernández, R. M., Castro, M., & Pedraz, J. L. (2008). Cell microencapsulation technology: Towards clinical application. *Journal of Controlled Release*, *132*, 76–83.

Muzzarelli, R. A. A. (2009a). Genipin-crosslinked chitosan hydrogels as biomedical and pharmaceutical aids. *Carbohydrate Polymers*, *77*, 1–9.

Muzzarelli, R. A. A. (2009b). Chitins and chitosans for the repair of wounded skin, nerve, cartilage and bone. *Carbohydrate Polymers*, *76*, 167–182.

Nugraha, B., Hong, X., Mo, X., Tan, L., Zhang, W., Chan, P. M., et al. (2011). Galactosylated cellulosic sponge for multi-well drug safety testing. *Biomaterials*, *32*, 6982–6994.

Qiu, Y., Mao, Z., Zhao, Y., Zhang, J., Guo, Q., Gou, Z., et al. (2012). Polycaprolactone scaffold modified with galactosylated chitosan for hepatocyte culture. *Macromolecular Research*, *20*, 283–291.

Rosas-Flores, W., Ramos-Ramírez, E. G., & Salazar-Montoya, J. A. (2013). Microencapsulation of *Lactobacillus helveticus* and *Lactobacillus delbrueckii* using alginate and gellan gum. *Carbohydrate Polymers*, *98*, 1011–1017.

Seo, S., Akaike, T., Choi, Y., Shirakawa, M., Kang, I., & Cho, C. (2005). Alginate microcapsules prepared with xyloglucan as a synthetic extracellular matrix for hepatocyte attachment. *Biomaterials*, *26*, 3607–3615.

Seo, S., Choi, Y., Akaike, T., Higuchi, A., & Cho, C. (2006). Alginate/galactosylated chitosan/heparin scaffold as a new synthetic extracellular matrix for hepatocytes. *Tissue Engineering*, *12*, 33–44.

Seo, S., Kim, I., Choi, Y., Akaike, T., & Cho, C. (2006). Enhanced liver functions of hepatocytes cocultured with NIH 3T3 in the alginate/galactosylated chitosan scaffold. *Biomaterials*, *27*, 1487–1495.

Strand, B. L., Morch, Y. A., Espevik, T., & Skjak-Braek, G. (2003). Visualization of alginate-poly-L-lysine-alginate microcapsules by confocal laser scanning microscopy. *Biotechnology and Bioengineering*, *82*, 386–394.

Tian, M., Chen, F., Ren, D., Yu, X., Zhang, X., Zhong, R., et al. (2010). Preparation of a series of chitooligomers and their effect on hepatocytes. *Carbohydrate Polymers*, *79*, 137–144.

Tian, M., Yang, Z., Kuwahara, K., Nimni, M. E., Wan, C., & Han, B. (2012). Delivery of demineralized bone matrix powder using a thermogelling chitosan carrier. *Acta Biomaterialia*, *8*, 753–762.

Tran, N. M., Dufresne, M., Duverlie, G., Castelain, S., Défarge, C., Paullier, P., et al. (2013). An appropriate selection of a 3D alginate culture model for hepatic Huh-7 cell line encapsulation intended for viral studies. *Tissue Engineering, A*, *19*, 103–113.

Villa, R., Cerroni, B., Viganò, L., Margheritelli, S., Abolafio, G., Oddo, L., et al. (2013). Targeted doxorubicin delivery by chitosan-galactosylated modified polymer microbubbles to hepatocarcinoma cells. *Colloids and Surfaces B: Biointerfaces*, *110*, 434–442.

Wang, J., Xiao, F., Zhao, Y., Chen, L., Zhang, R., & Guo, G. (2010). Cell proliferation and thermally induced cell detachment of galactosylated thermo-responsive hydrogels. *Carbohydrate Polymers*, *82*, 578–584.

Xu, Y., Li, L., Wang, H., Yu, X., Gu, Z., Huang, C., et al. (2013). In vitro cytocompatibility evaluation of alginate dialdehyde for biological tissue fixation. *Carbohydrate Polymers*, *92*, 448–454.

Yang, J., Gotob, M., Ise, H., Cho, C. S., & Akaike, T. (2002). Galactosylated alginate as a scaffold for hepatocytes entrapment. *Biomaterials*, *23*, 471–479.

Yang, N., Chen, L., Yang, M., Bi, S., He, X., Zhu, Z., et al. (2012). In vitro study of the interactions of galactosylated thermo-responsive hydrogels with cells. *Carbohydrate Polymers*, *88*, 509–516.

Yin, C., Chia, S. M., Quek, H. C., Yu, H., Zhuo, R., Leong, K., et al. (2003). Microcapsules with improved mechanical stability for hepatocyte culture. *Biomaterials*, *24*, 1771–1780.

Zhang, J., Tang, C., & Yin, C. (2013). Galactosylated trimethyl chitosanecysteine nanoparticles loaded with Map4k4 siRNA for targeting activated macrophages. *Biomaterials*, *34*, 3667–3677.

Zhang, W., Zhao, S., Rao, W., Snyder, J., Choi, J. K., Wang, J., et al. (2013). A novel core–shell microcapsule for encapsulation and 3D culture of embryonic stem cells. *Journal of Materials Chemistry B*, *1*, 1002–1009.

Zhang, Y., Shi, X., Han, B., Gu, J., Chu, X., Xiao, J., et al. (2012). The influence of membrane molecular weight cutoff on a novel bioartificial liver. *Artificial Organs*, *36*, 86–93.

Zheng, D., Duan, C., Zhang, D., Jia, L., Liu, G., Liu, Y., et al. (2012). Galactosylated chitosan nanoparticles for hepatocyte-targeted delivery of oridonin. *International Journal of Pharmaceutics*, *436*, 379–386.

Zhou, N., Zan, X., Wang, Z., Wu, H., Yin, D., Liao, C., et al. (2013). Galactosylated chitosan-polycaprolactone nanoparticles for hepatocyte-targeted delivery of curcumin. *Carbohydrate Polymers*, *94*, 420–429.

Zhu, J. H., Wang, X. W., Ng, S., Quek, C. H., Ho, H. T., Lao, X. J., et al. (2005). Encapsulating live cells with water-soluble chitosan in physiological conditions. *Journal of Biotechnology*, *117*, 355–365.